Research Article

For reprint orders, please contact: reprints@futuremedicine.com

Regenerative Medicine

Microsphere-based gradient implants for osteochondral regeneration: a long-term study in sheep

Background: The microfracture technique for cartilage repair has limited ability to regenerate hyaline cartilage. **Aim**: The current study made a direct comparison between microfracture and an osteochondral approach with microsphere-based gradient plugs. **Materials & methods**: The PLGA-based scaffolds had opposing gradients of chondroitin sulfate and β-tricalcium phosphate. A 1-year repair study in sheep was conducted. **Results**: The repair tissues in the microfracture were mostly fibrous and had scattered fissures with degenerative changes. Cartilage regenerated with the gradient plugs had equal or superior mechanical properties; had lacunated cells and stable matrix as in hyaline cartilage. **Conclusion**: This first report of gradient scaffolds in a long-term, large animal, osteochondral defect demonstrated potential for equal or better cartilage repair than microfracture.

Keywords: cartilage regeneration • chondroitin sulfate • gradients of signals • osteochondral tissue engineering • microfracture • microsphere-based scaffold

Neethu Mohan[1,2], Vineet Gupta[3], Banu Priya Sridharan[3], Adam J Mellott[1], Jeremiah T Easley[4], Ross H Palmer[4], Richard A Galbraith[5], Vincent H Key[6], Cory J Berkland[1,3,7] & Michael S Detamore*[,1,3]

[1]Department of Chemical & Petroleum Engineering, University of Kansas, Lawrence, KS 66045, USA
[2]Biomedical Technology Wing, Sree Chitra Tirunal Institute for Medical Sciences & Technology, Trivandrum, Kerala 695011, India
[3]Bioengineering Graduate Program, University of Kansas, Lawrence, KS 66045, USA
[4]Preclinical Surgical Research Laboratory, College of Veterinary Medicine & Biomedical Sciences, Colorado State University, Fort Collins, CO 80523, USA
[5]Lawrence Memorial Hospital, Lawrence, KS 66044, USA
[6]University of Kansas Medical Center, Kansas City, KS 66160, USA
[7]Department of Pharmaceutical Chemistry, University of Kansas, Lawrence, KS 66045, USA
*Author for correspondence:
Tel.: +1 785 864 4943
Fax: +1 785 864 4967
detamore@ku.edu

Articular cartilage has limited healing capabilities, and may contribute to the development of osteoarthritis if left untreated after an impact injury. To prevent the development of osteoarthritis, several techniques have been developed to stimulate cartilage regeneration, which include abrasion arthroplasty, subchondral drilling, microfracture, autologous chondrocyte implantation (ACI), matrix associated autologous chondrocyte implantation (MACI) and implantation of osteochondral autografts and allografts [1]. Abrasion arthroplasty, subchondral drilling and microfracture strategies induce the formation of fibrocartilage, which helps to alleviate painful symptoms and to restore the function of affected joints; however, fibrocartilage has a limited life span and poor mechanical performance in comparison to articular cartilage [2,3]. While there is a greater chance of producing articular cartilage in the injured area by ACI, the technique has several disadvantages, which include the need for two surgical procedures, generation of a large quantity of chondrocytes based on the defect size and issues with graft fixation, delamination and periosteal hypertrophy [4]. Similarly, MACI is a technique that seeds patient-grown chondrocytes on a biomaterial for implantation into the patient; however, MACI is still limited by the need for two surgical procedures, cost and generation of chondrocytes based on defect parameters [4].

In addition, implantation of osteochondral autografts and allografts has been used to treat full thickness osteochondral defects; however, the harvest procedures for autografts are associated with an increased risk of morbidity at the donor site. Further concerns regarding implantation of osteochondral autografts and allografts include availability of donor site tissue, geometry mismatch of graft tissue and inadequate bonding of the graft tissue to the surrounding cartilage of the defect [5,6]. An advantageous strategy would be to implant a biodegradable material that promotes biochemical cues that stimulate osteochondral regeneration without the need to induce additional injuries, or implant autografts or allografts. There are numerous

Future Medicine part of fsg

other biomaterial implants that have been reported for osteochondral defects and that have even been evaluated in clinical trials [7–9]. These plugs are generally biphasic in nature, meaning disparate cartilage and bone regions with a sharp interface in-between, where delamination of the cartilage layer could become a concern. Moreover, it would generally be difficult for these approaches to encapsulate growth factors in the future for product life cycle management.

We have previously succeeded in regenerating osteochondral defects in rabbit femoral condyles with microsphere-based gradient plugs, where we overcame plug limitations by releasing 'raw materials' for the tissue and growth factors, and by creating a seamless osteochondral interface in the material [10]. While rabbits are an appropriate small-animal screening tool and our results have been encouraging, a large-animal model is necessary for translating a cartilage repair technology to the clinic, as is a comparison to the current standard of care, which is widely accepted to be microfracture. The current study thus presents the first evaluation of the microsphere-based gradient plugs in a large animal model, with a long-term end point of 1 year. The hypothesis of the current study was that microsphere-based gradient plugs with opposing continuous gradients of chondroitin sulfate and β-tricalcium phosphate (β-TCP) in osteochondral defects would provide cartilage regeneration superior to that achieved by microfracture in chondral-only defects in a sheep model.

The primary purpose of this study was to evaluate the aforementioned hypothesis, thereby evaluating microsphere-based gradient plugs for the first time in a large-animal cartilage repair study and in a translational context with a current standard-of-care control. The secondary purpose was to demonstrate the feasibility and proof of concept of adding a metered dose of growth factor to an osteochondral implant immediately preceding implantation in the operating room, which was evaluated in two pilot groups with the microsphere-based gradient plugs.

Materials & methods

Materials

PLGA (50:50 lactic acid: glycolic acid, ester end group, M_w 106 KDa, intrinsic viscosity 0.6–0.8 dl/g) and PLGA (75:25 lactic acid: glycolic acid, ester end group, M_w112 KDa, intrinsic viscosity 0.6–0.8 dl/g) were obtained from Lakeshore Biomaterials™ (AL, USA). TGF-β3 (recombinant human, *Escherichia coli* derived) and IGF-1 (recombinant human, *E. coli* derived) were obtained from PeproTech Inc. (NJ, USA). Chondroitin sulfate A sodium salt (CS) (from bovine trachea) and β-TCP were obtained from Sigma-Aldrich (MO, USA). Sodium bicarbonate was obtained from Fisher Scientific (PA, USA). All reagents and organic solvents utilized were of cell culture or ACS grade.

Fabrication of microspheres

Two different sets of microspheres were fabricated for the current study: Chondrogenic microspheres (PLGA-CS-$NaHCO_3$; 77.5:20:2.5) and osteogenic microspheres (PLGA-β-TCP; 90:10). Chondrogenic microspheres were fabricated by adding 20% w/v CS and 2.5% w/v $NaHCO_3$ to 77.5% w/v PLGA (50:50 lactic acid: glycolic acid, ester end group, intrinsic viscosity 0.6–0.8 dl/g) dissolved in dichloromethane (DCM; 20% w/v). $NaHCO_3$ was dissolved in a minimum volume of distilled (DI) water to which CS powder was added to obtain a uniform viscous solution that was mixed with PLGA dissolved in DCM. The final mixture was sonicated at 50% amplitude for 2 min. The rationale for the inclusion of $NaHCO_3$ was to buffer the acidic byproducts of PLGA, a well-known technique established in the 1990s by Agrawal and Athanasiou [11].

Osteogenic microspheres were fabricated by adding 10% w/v of β-TCP to 90% w/v PLGA (75:25 lactic acid: glycolic acid, ester end group, intrinsic viscosity 0.6–0.8 dl/g) in DCM (20% w/v). β-TCP powder was added to PLGA dissolved in DCM and sonicated at 50% amplitude for 2 min. The slower degrading PLGA formulation was chosen for the bone side of the construct to provide longer lasting support, as preliminary data from a 3-month pilot osteochondral defect study in sheep demonstrated that the PLGA formulation used in our previous rabbit studies degraded too quickly to maintain structure. $NaHCO_3$ was not included as our experience *in vitro* has demonstrated a buffering effect provided by the β-TCP.

Two different batches of monodisperse microspheres were prepared using the aforementioned emulsions of PLGA-CS-$NaHCO_3$ and PLGA-β-TCP according to our previously reported technology [12–14]. Briefly, uniform polymer droplets were created by introducing regular jet instabilities in the polymer stream through acoustic excitation via an ultrasonic transducer. An annular carrier nonsolvent stream (0.5–2% w/v polyvinyl alcohol [PVA] in DI water) surrounding the droplets was produced using a nozzle, coaxial to the needle. The polymer/carrier streams flowed into a beaker containing the nonsolvent. The polymer droplets were stirred for 3–4 h to allow for solvent evaporation. Afterward, droplets were filtered and rinsed with DI water to remove residual PVA. Microspheres were frozen at -20°C and lyophilized for 48 h. Monodisperse microspheres with size within the range of 280–400 μm were fabricated for the current study.

Fabrication of gradient scaffolds

Gradient scaffolds were prepared using our previously reported technology [12–15]. Briefly, 50 mg of lyophilized chondrogenic microspheres and 100 mg of osteogenic microspheres were dispersed in DI water, and separately loaded into two syringes. Suspensions were pumped at opposing flow rates into cylindrical polypropylene molds (diameter = 6 mm) in a controlled manner using programmable syringe pumps (PHD 22/2000, Harvard Apparatus, Inc., MA, USA). DI water was filtered through the bottom of the mold, while microspheres were stacked in the mold until a height of 6 mm was reached. A gradient profile was used for engineering scaffolds in which chondrogenic microspheres comprised the top quarter (1.5 mm), followed by a (1.5 mm) linear transition from chondrogenic microspheres to osteogenic microspheres, and the bottom half (3 mm) were comprised only osteogenic microspheres. Options to sinter microsphere-based scaffolds include heat [16], carbon dioxide [17,18] and solvent/nonsolvent sintering [13]. In the current study, the stacked microspheres were sintered together using ethanol-acetone (95:5 v/v) for 45 min and were further lyophilized at -20°C for 48 h. The resulting scaffolds were 6 mm in diameter and 6 mm height. They were ethylene oxide sterilized in sterile pouches and transported to Colorado State University for implantation.

Surgical procedures for implantation of gradient scaffolds (group I) & microfracture (group II) in sheep femoral condyles

Details of sheep used for the study

Eighteen (18) skeletally mature (>3.5 years of age) female Rambouillet × Columbia cross sheep were used for the current study. The weight of animals is tabulated in the Box 1. All procedures were approved by the CSU IACUC protocol #11-3150 and KU IACUC protocol #175-14. Animals received one of two types of primary treatments. Group I consisted of 12 animals (knee numbers: D01–D12) that received gradient implants and group II consisted of six animals (knee numbers: D13–D18) that underwent a microfracture procedure.

Subgroups in group I: sheep that received gradient scaffolds

In group I, osteochondral defects (6 mm diameter × 6 mm depth) were created in both the medial femoral condyles (MFCs) and lateral femoral condyles (LFCs) of the right knee joints of the sheep [19]. Three subgroups were analyzed in group I. In group I–A, the sheep received gradient plug implants (n = 6, knee numbers: D01–D06). In group I–B, the sheep received gradient plug implants infiltrated with TGF-β3 (n = 3, knee numbers: D07–D09). In group I–C, the sheep received gradient plug implants infiltrated with IGF-1 (n = 3, knee numbers: D10–D12). The scaffold structure and the study design are schematically represented in Figure 1.

Box 1. Animal ID and weight of each animal at the time of implantation.

Animal ID: weight in kg

- D01: 90
- D02: 73
- D03: 87
- D04: 80
- D05: 90
- D06: 78
- D07: 89
- D08: 76
- D09: 87
- D10: 85
- D11: 81
- D12: 82
- D13: 70
- D14: 85
- D15: 81
- D16: 88
- D17: 85
- D18: 76

Details of anesthesia during surgery

For all animals of groups I and II, anesthesia was induced with intravenous ketamine and propofol and maintained with inhalant isoflurance and oxygen via endotracheal intubation. Sheep were placed in dorsal recumbency; the skin over the right knee joint was prepared for aseptic surgery using alternating scrubs of povidone-iodine and alcohol followed by sterile application of regional surgical drapes. A lateral parapatellar arthrotomy was performed and the medial and LFCs exposed.

Defect size & implantation of gradient scaffolds in group I animals

In group I, a custom depth-limiting drill guide was positioned perpendicular to the cartilage surface and impacted through the cartilage and into subchondral bone using a mallet. Progressively sized drill bits were used through the drill guide to create one sharp edged, 5.8 mm diameter × 6 mm deep osteochondral defect each in the medial and lateral femoral condyles. A #11 scalpel blade was used as needed to trim the cartilage edges. The gradient plugs used in group I–A were wetted with sterile normal saline before implantation. The gradient plugs used in group I–B received a drop-wise addition of 70 µl of TGF-β3 containing 10 mM citric acid with 0.1% BSA (Fisher Scientific, USA), resulting in a total dose of 1 µg TGF-β3 per plug. The con-

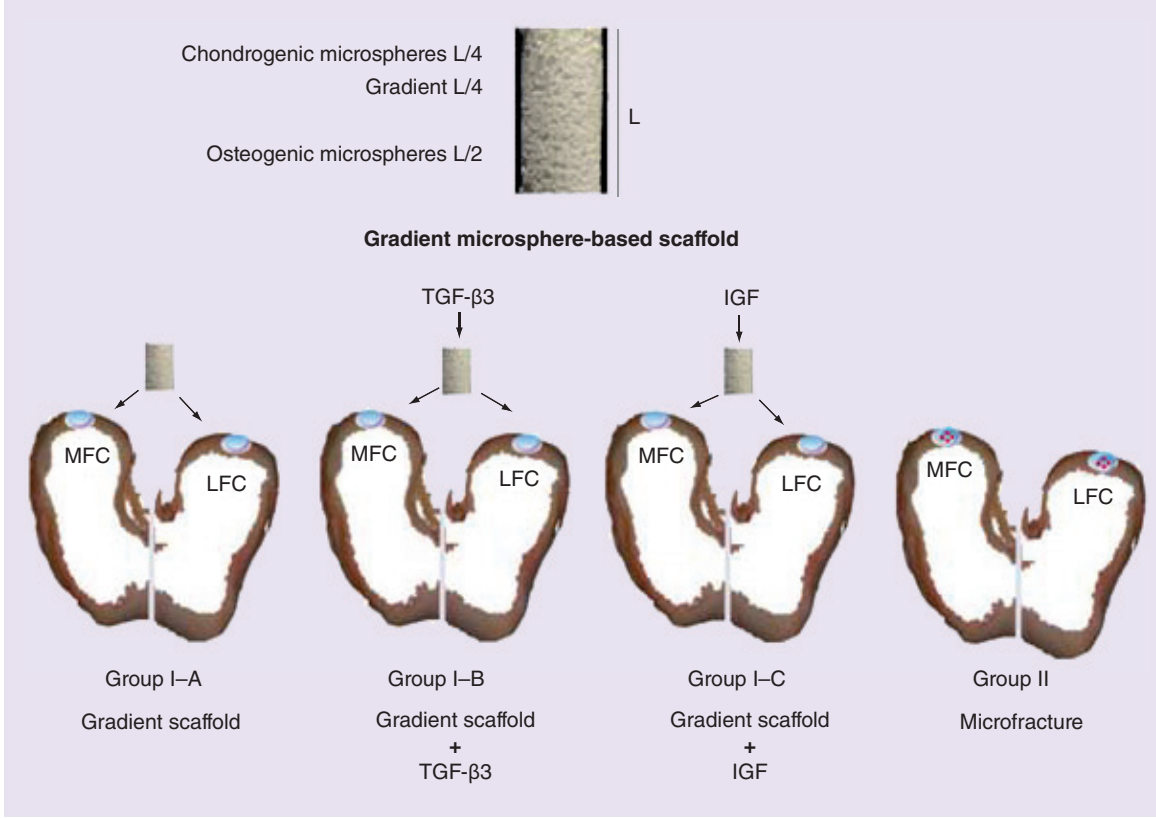

Figure 1. A schematic representation of microsphere-based gradient scaffold and the various groups for implantation. Gradient scaffolds were implanted into critical size osteochondral defects (D = 6 mm × H = 6 mm) in the lateral and medial femoral condyles of knee joints of group I animals. Group I–A received only the gradient scaffold (n = 6), and was the primary test group. Group I–B was a pilot group, where 1 μg TGF-β3 was added to the scaffold in the operating room immediately prior to implantation (n = 3). Similarly, 0.5 μg IGF-1 was added to the scaffold immediately prior to implantation in pilot group I–C (n = 3). Microfracture procedure was performed in group II animals (n = 6) following induction of full-thickness, chondral-only defects (D = 6 mm). The cartilage regeneration was evaluated 1 year post-implantation.
LFC: Lateral femoral condyle; MFC: Medial femoral condyle.

centration of the TGF-β3 was estimated based on our calculations from gradient implants used for the osteochondral regeneration in critical size defects in rabbits and total volume of the defect site in sheep [20]. The gradient plugs used in group I–C received a drop-wise addition of 60 μl of DI water containing a total dose of 0.5 μg of IGF-1 per plug. The dose of the IGF was determined based on the amount of IGF used for cartilage regeneration in rabbits as well as in other large animals reported in the literature [21,22]. In groups I–B and I–C, growth factors were added from a 100 μl pipette with a sterile tip in the operating room immediately prior to implantation. Material gradient implants were manually placed into each of the defects by press fitting method; care was used to align the implant with the axis of the drilled defect. The scaffold stability, congruency with surrounding cartilage and ease of insertion were noted for each implant.

Due to differences in relative diameters of scaffolds and drill bits compared with a preliminary study with six sheep, where no crumbling of defects was observed, there were some scaffolds that required excessive force to press-fit into the defect, resulting in some degree of crumbling. We observed an estimate of less than 5% crumbling in the following samples: LFC of sheep #D01, MFC of sheep #D03, MFC of sheep #D07, MFC of sheep #D08 and MFC and LFC of sheep #D09, and 5–10% crumbling in the MFC in sheep D11.

Microfracture procedure for group II animals

For group II, the sheep were subjected to a microfracture procedure (n = 6, knee numbers: D13–D18), in the MFC and LFC of right knee joints. A standardized circular chondral lesion (6.0 mm in diameter) was created in the MFCs and LFCs with a fine 6.0 mm punch. The cartilage within these limits was abraded down through the calcified cartilage layer with a size 0 currette taking care not to penetrate the subchondral bone plate or provoke bleeding from the lesion bed. Once the full-thickness cartilage lesion was created leaving

intact subchondral bone, a custom 1.6 mm (0.062") micropick and mallet were used to create four holes (~2 mm from defect edge and apart from one another) into the subchondral bone to a depth of 5–8 mm. The amount of bleeding from the micropick sites was scored 0–4 (0 = no bleeding; 4 = obvious bleeding from five sites).

For animals of both groups, the joint capsule and fascia were approximated with interrupted sutures of #2/0-Polysorb™ suture material in an interrupted pattern. Subcutaneous tissues were closed in a simple continuous pattern using #2/0-Polysorb™ suture material, while skin closure was apposed in an interlocking pattern using #2/0 Nylon. Operative time was approximately 35 min.

Post operative care for animals

Following implantation of scaffolds, group I sheep were housed indoors for two weeks. At the end of 2 weeks, all sheep were moved to an outdoor paddock with access to a three-sided shelter. Sheep remained there for the rest of the convalescence period and were allowed to exercise at will. An effort was made to approximate the nonweight bearing requirement of human microfracture patients by keeping the sheep housed indoors for 4 weeks, after which they were allowed to join the group I sheep in the outdoor paddock. This approach was chosen given that bed rest and continuous passive motion for several weeks was not a practical option, and using a sling to prevent weight-bearing would not have been a true approximation, difficult to practically implement and may raise ethical concerns.

Progression of cartilage regeneration was evaluated using MRI at 4 months for group I and group II, as described below. All groups had a single end point of 52 weeks, and sheep were humanely euthanized by intravenous barbiturate overdose (Pentobarbitone sodium, 88 mg/kg) according to the guidelines set forth by the American Veterinary Medical Association in 2007. The joints were retrieved, and MFCs and LFCs were morphologically scored and photographed. All of the samples were analyzed for mechanical properties followed by histological processing and evaluation, as described below.

MRI analysis at 4 months

Progression of cartilage regeneration was evaluated using 1.5 T MRI (GE Signa HD × T) at 4 months for group I (n = 3 knees) and group II (n = 3). The sheep were placed under general anesthesia prior to imaging. T2/sagittal, PD Fat-Sat/3-plane, Gradient echo/sagittal MR imaging sequences were performed on all treated knees. The MRIs were scored blindly by a boarded veterinary radiologist from Colorado State University for articular surface defect fill, the quality of regenerated cartilage, subchondral trabecular bone defect fill, subchondral trabecular bone sclerosis and edema, joint effusion, synovitis and joint capsule thickening.

Morphological analysis of the retrieved implants

After retrieval, implants were scored blindly by three independent co-authors. The scoring was carried out for macroscopic observations based on different parameters such as the presence of repair tissue, presence of implant at the defect site, edge integration at the boundaries of newly regenerated tissue and the native cartilage, smoothness of the repair surface, degree of filling at the cartilage surface, color of the regenerated cartilage and the percent of repair tissue relative to the total area. The scoring criteria are represented in Box 2. The joints were photographed and processed for mechanical testing.

Mechanical testing

Femurs were retrieved, wrapped in gauze, soaked in PBS and stored at -20°C until the day of testing. Each frozen femur was thawed at room temperature for 1 h in a normal saline solution (0.15 M NaCl) containing enzymatic inhibitors (EDTA, 2 mM; benzamidine HCl, 5 mM; N-ethyl malemide, 10 mM; and PMSF, 1 mM) [23]. Afterward, MFCs and LFCs were separated with a handheld hacksaw by cutting the femurs along the patellar surface. Each MFC and LFC was affixed to a stainless steel platform using cyanoacrylate adhesive, placed in a custom made bath depicted in Supplementary Figure 2 and submerged in the saline solution with protease inhibitors. The temperature of the bath was maintained at 37°C at all times during the testing using an immersion heater. A uniaxial testing apparatus (Instron 5848 Microtester, MA, USA) was used for both cartilage thickness measurement and unconfined indentation stress relaxation tests. A total of three sites were tested to determine the thickness, whereas indentation was performed only at the central region of the implant site. Thickness was measured via a thin needle that was inserted into the implant site perpendicularly to the specimen surface at a constant rate of 0.5 mm/min. During this thickness measurement process, the force and displacement were measured, and needle movement was terminated when the force reached 5 N. Specimen thickness was determined using a force displacement curve. A change in slope indicated the point where the needle contacted the subchondral bone [24]. For indentation stress relaxation testing, the tare-loaded (0.01 N) implant site was sub-

Box 2. Morphology scoring parameters for the regenerated tissue and associated numeric score.

Gross morphology scoring parameters

- Repair tissue or scaffold present in the implant site:
  - Full presence 2
  - Partial 1
  - None 0
- Edge integration (new tissue relative to native cartilage):
  - Full 2
  - Partial 1
  - None 0
- Smoothness of repair surface:
  - Smooth 2
  - Intermediate 1
  - Rough/missing 0
- Cartilage surface degree of filling:
  - Flush 2
  - Slight depression 1
  - Depressed/overgrown 0
- Color of cartilage (opacity /translucency of repair tissue):
  - Translucent 2
  - Opaque 1
  - Missing 0
- Amount of repair tissue relative to total area of defect:
  - Estimated percentage present in defect

jected to 10% strain (at a ramp rate of 0.05%/s) using a solid flat tip aluminum indenter (1.5 mm diameter) and then allowed to relax for a period of 1000 s, which was determined in preliminary tests to be a sufficient period of time for relaxation. After the mechanical testing, the condyles were processed for histological evaluation.

Finite element analyses

To curve-fit the unconfined compression stress relaxation response of test specimens, a finite element analyses was performed in which cartilage was modeled as a biphasic material [25]. The porous extracellular matrix was described by a solid mixture of a neo-Hookean ground matrix reinforced by a continuous, random distribution of fibril bundles sustaining tension only; the hydraulic permeability was assumed constant [26–28]. The model had a total of five material constants: Aggregate modulus (E) and Poisson's ratio (ν) for the neo-Hookean solid, the fibril modulus (k_{si}) and the power-law exponent β for the spherical fiber distribution, and the constant hydraulic permeability k. It was assumed *a priori* that ν = 0 (for the porous ground matrix due to the compressibility of the pore space) and β = 2 (to produce a linear tensile response in the range of small strains, consistent with the known behavior of cartilage) so that the parameter optimization was only performed on E, k_{si} and k [27].

The finite element analyses for curve-fitting the experimental data in unconfined compression, and modeling the contact between indenter and the specimen, were performed with the open-source program FEBio available in the public domain [29]. Curve-fitting was performed using FEBio's built-in least-squares parameter optimization routine, based on the Levenberg-Marquardt algorithm. The contact was modeled using an impermeable flat indenter with a diameter of 1.5 mm and a cylindrical tissue of diameter of 11 mm, and 1 mm thick. Due to symmetry, only a wedge of the geometry was modeled. The indenter produced a compressive deformation of 10% of the thickness. The contact interface between the indenter and the construct was assumed to be frictionless. The bottom of the construct was fixed to a rigid impermeable substrate. Fluid was allowed to escape from the free boundaries not in direct contact with the indenter. The model consisted of 784 hexahedral 8-node elements and 1727 nodes. The mesh was biased along the thickness to produce thinner elements near the top and bottom surfaces; a coarser mesh was also employed at the far ends along the length. FEM results were visualized using the FEBio Postview environment [29].

Histological analysis

Sheep knee samples were fixed in 10% buffered formalin phosphate (Fisher Scientific, NJ, USA) and decalcified using Cal Rite (Richard Allen Scientific Inc., MI, USA) for 3 weeks. Before processing, the samples were rapidly decalcified for 2 h using RBD (Rapid Bone Decalcifier, American Mastertech Scientific Inc, CA, USA). The samples were dehydrated in ethanol and processed for paraffin embedding. Sections of 5 µm thickness from the center of the defect site were cut using a microtome (Thermo Scientific, Microm HM 355S). The sections were further deparaffinized and rehydrated for staining. The sections were stained with hematoxylin-eosin and Safranin-O (Saf-O). A modified O'Driscoll scoring system (consisting of parameters listed in Box 3) was used for the analysis [30–32]. Histological scoring was performed by three independent co-authors and the mean was calculated. The sections were also stained with Sudan black to identify whether polymer was present at the defect site.

Statistical analysis

Statistical analyses were performed using a single factor analysis of variance (ANOVA) with a Tukey's *post hoc* test using GraphPad Prism version 5.02 for Windows, (GraphPad software, CA, USA). All quan-

titative results were expressed as the mean ± SD. Values of $p < 0.05$ were considered significant.

Results

Function (ability to walk)

After recovering from surgery, sheep were able to walk on their own. Once transferred to the small pen, the sheep moved normally and exhibited no signs of lameness at any point in the 12-month study duration. After the initial period in pens, the sheep were able to roam, run and jump freely (i.e., normal behavior).

MRI analysis at 4 months post-implantation

The joints were imaged and representative figures are shown in Figure 2. The MRI grading scale, average scores for the LFCs and MFCs of sheep at 4 months post-implantation and highlights of the scoring results are listed in Table 1. In the unoperated control native knee joint, no abnormalities were detected. The cartilage layer on top of the medial and lateral articular surfaces was well defined in native joints. Cartilage regeneration was observed in all samples at 4 months post-implantation, and defect areas were generally well contained. The average scores are listed in Box 1, and the differences were not statistically significant. Of all of the groups examined for tissue fill, the microfracture group received a highest average score of 4 for the MFCs and the lowest average score of 2 for the LFCs. Defects in the MFCs and LFCs treated with microfracture exhibited faster fill of the defect in the bone, but it is important to recall that defects treated with microfracture were only chondral defects with small holes made in the subchondral bone. In contrast, gradient scaffolds were implanted in osteochondral defects (6 mm depth) and exhibited slower bone regeneration. However, defects treated with microfracture received a higher average score for bone sclerosis, whereas defects treated with material gradient implants (no growth factors) received the lowest score for bone sclerosis. Moderate edema was observed in MFCs while negligible levels of edema were observed in LFCs in all groups.

Defects treated with material gradient scaffolds alone displayed isointense (normal) to hypointense signals on 3D SPGR. The intensity of the articular cartilage signal on 3D SPGR weighted sequences varied between hypointense to normal in treated defects from the TGF-β3 group, the IGF group and the microfracture group in the MFCs; whereas the signal intensity for the LFCs varied between normal and hyperintense for treated defects from the TGF-β3 group, the IGF group and the microfracture group.

The intensity of the articular cartilage signal on PD-weighted sequences displayed either normal signal intensity or hypointense to normal signal intensity in sheep from gradient scaffold-only group. Sheep that received IGF-1 treated scaffolds displayed normal signal intensity, and sheep that received TGF-β3 treated scaffolds or that were treated with microfracture displayed hypointense/hyperintense to normal signals.

Gross morphological assessment

Gross examinations of the knee joints revealed no evidence of skin inflammation or infection. The total morphological scores and the percentage of tissue fill at the defect site are graphically represented in Figure 3A & B. The gross morphology images of both LFCs and MFCs in all sheep, 1-year post-implantation, are shown in Supplementary Figure 1. No signs of degeneration were noted on the opposing surfaces. All of the sheep that received gradient scaffolds alone (n = 6) displayed total tissue fill above 80% on both condyles, except one animal, #D01, which displayed a tissue fill of 55 and 40% on the LFC and the MFC, respectively. The average total repair tissue fill in group I–A was 76 ± 18% and 84 ± 16% in the MFCs and LFCs, respectively. Defects implanted with the gradient scaffold-only received total morphological scores ranging from 6 to 10 across all examined condyles. The gradient scaffold-only group LFCs received an average score of 8.0 ± 1.4, where new cartilage appeared either translucent or opaque. A slight depression was observed in newly formed cartilage in both condyles with the depression appearing centrally in LFCs and axially in MFCs. In all except one of the LFCs, #D01, the cartilage surface appeared to be smooth. Furthermore, the new tissue integrated with the native tissue in about 70% of the LFCs and new tissue incompletely integrated in MFCs.

Sheep that received gradient scaffolds infiltrated with TGF-β3 (n = 3) had an average percentage tissue fill of 78 ± 22% in the MFCs and 87 ± 8% of repair tissue in LFCs. The newly formed cartilage was translucent in all except one of the condyles #D09 MFC, where it was opaque in appearance. The surface was not smooth in 50% of the condyles #D07 MFC, #D08 LFC and #D09 LFC. The other three condyles displayed translucent and smooth surfaces. The dot plot (Figure 3C) shows the distribution of total morphological scores ranged from 4 to 10 in the TGF-β3 treated gradient scaffold group with the defect fill ranging between 80 and 98% (Figure 3D) for all except one animal, #D09, which had a defect fill score < 60% in the LFC. During necropsy, the axial edge appeared roughened at the MFC and yellow pus was observed at the marrow cavity in sheep #D07. In sheep #D09, signs of osteoarthritis were observed on the patella and outer regions of cartilage not involved with the defect. Infections not related to the implant might have influenced

Box 3. Histology scoring parameters and associated numeric score.

Nature of predominant tissue

- Cellular morphology:
  - Hyaline cartilage 4
  - Mostly hyaline cartilage 3
  - Mixed hyaline and fibrocartilage 2
  - Mostly fibrocartilage 1
  - Some fibrocartilage and mostly nonchondrocytic cells 0
- Safranin O staining:
  - Normal or nearly normal 3
  - Moderate 2
  - Slight 1
  - None 0
- Structural characteristics:
  - Normal 2
  - Slight disruption, including cysts 1
  - Severe disintegration, disruptions 0
- Thickness:
  - Similar to the surrounding cartilage 3
  - Greater than the surrounding cartilage 2
  - Less than the surrounding cartilage 1
  - No cartilage 0
- Bonding:
  - Bonded at both ends of graft 2
  - Bonded at 1 end or partially at both ends 1
  - Not bonded 0
- Reconstruction of subchondral bone:
  - Normal or reduced subchondral bone reconstruction 2
  - Minimal subchondral bone reconstruction 1
  - No subchondral bone reconstruction 0
- Degenerative changes: graft
  - Normal cellularity 2
  - Slight hypocellularity 1
  - Moderate hypocellularity or hypercellularity 0
- Chondrocyte clustering:
  - No clusters 2
  - < 25% of the cells 1
  - 25 - 100% of cells 0
- Degenerative changes: adjacent cartilage:
  - Normal cellularity, no clusters, normal staining 3
  - Normal cellularity, mild clusters,
  - moderate staining 2
  - Mild/moderate cellularity, moderate clusters,
  - moderate hypocellularity, slight staining 1
  - Severe hypocellularity and degeneration, poor or no staining 0
- Structural integrity of regenerated cartilage:
  - Normal 2
  - Slight disruption, including cysts 1
  - Severe disintegration, disruptions 0
- Inflammatory response in subchondral bone:
  - None/mild 2
  - Moderate 1
  - Severe 0

Total maximum possible score: 28

The grading system was modified from the previous reported system of O'Driscoll *et al.* [30,31].

the regeneration of cartilage in these animals (#D07 and #D09).

The group that received gradient scaffolds infiltrated with IGF-1 (n = 3) had average tissue fill scores of 57 ± 10% and 75 ± 15% in the LFCs and MFCs, respectively. The distribution of total morphology scores ranged from 3 to 6 and scores for tissue fill ranged from 40 to 85%. In most of the condyles, the newly formed tissue appeared opaque and rough, especially in the MFCs. The appearances of depressions in newly formed tissues were significant in MFCs and slight in LFCs.

The group that was treated with microfracture (n = 6) had an average percentage tissue fill of 78 ± 12% in the MFCs and 76 ± 21% of repair tissue in the LFCs. The distribution of total morphological scores ranged from 2.5 to 9.6 and tissue fill scores ranged from 42 to 98%. The MFCs exhibited a greater abundance of repair tissue in the defect site, which appeared opaque, than the LFCs. Moreover, in some of the LFCs, the repair tissue was translucent rather than opaque. In both the MFCs and the LFCs, the repair tissue was slightly depressed. The repair tissue integrated only partially with the native tissue. In addition, most of the samples had multiple fissures of smaller size or islands of cartilage throughout the regenerated surface (Supplementary Figures 4 & 5).

Mechanical testing of repair tissue

The aggregate modulus, fiber modulus and permeability of regenerated tissue for all of the groups are represented graphically in Figure 4. The aggregate moduli (H_A), determined by curve fitting the indentation stress relaxation data, were 38 ± 15 kPa (medial condyles) and 64 ± 31 kPa (lateral condyles) for the untreated native tissue (control) samples. Sheep treated with the gradient scaffold only exhibited aggregate moduli of 12 ± 19 kPa (medially) and 9.2 ± 9.2 kPa (laterally) with the lateral condyles having significantly lower values ($p < 0.05$) than the untreated lateral samples. No significant differences in aggregate moduli were observed in any other groups. Data for the medial condyles in gradient scaffolds treated with TGF-β3 could not be determined from the curve fitting experiments because the R^2 value was less than 0.65. The microfracture group displayed significantly higher ($p < 0.05$) permeability values in the LFCs at 1.0 ± 1.3 $mm^4/N.s$ than in the control group (0.023 $mm^4/N.s$). However, no significant differences were found between the MFCs of the control group and the microfracture group. Additionally, no significant differences were observed among the groups with respect to fiber modulus. The fiber moduli were observed to be 3.3 ± 3.1 kPa (medially) and 8.3 ± 9.6 kPa (laterally) in the native joint of

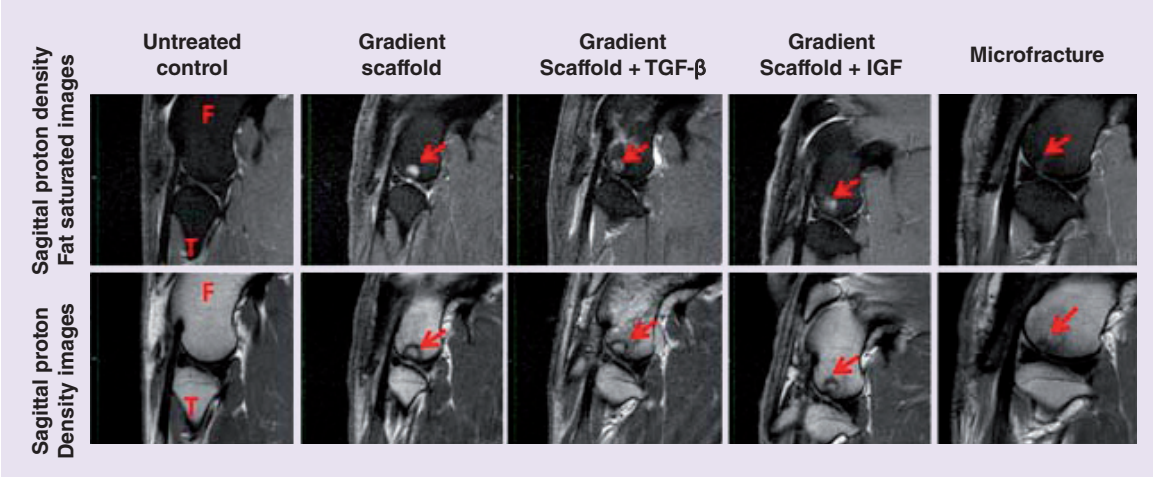

Figure 2. Representative 1.5 T MRI images of femoral condyles of sheep 4 months post-implantation, showing progress of cartilage and bone regeneration. A total of three knees were imaged for each group. The arrows point to the defect site on the images. F and T denote femur and tibia respectively. Cartilage regeneration was observed in all of the samples at 4 months, and defect areas were generally well-contained. The microfracture group showed faster defect fill in the bone, due to the microfracture procedure being only a chondral defect with small holes made in the subchondral bone, in contrast to the gradient scaffolds, which filled osteochondral defects 6 mm in depth and likely had remnants of the polymer remaining at the time these MRIs were taken. From left to right, the representative samples are from the following animals: control, D02 lateral femoral condyle (LFC), D09 LFC, D10 LFC and D15 LFC.

the control group, whereas the corresponding values in the gradient scaffold-only group, IGF group, TGF-β3 group and the microfracture group were 6.1 ± 5.2 kPa and 4.8 ± 5.0 kPa, 3.7 ± 2.5 kPa and 2.9 ± 1.6 kPa, 6.7 ± 5.3 kPa and not determined and 3.1 ± 1.9 kPa and 1.3 ± 1.5 kPa, respectively.

Histology

A modified O'Driscoll scoring system based on parameters listed in Box 3 was used to assess the cellular features and formation of new tissue in the defect site. Representative images of H&E and Saf-O staining are displayed for the gradient-only, microfracture groups and untreated control in Figure 5 and for the IGF and TGF-β3 groups in Figure 6. The average histological score received for the LFC and MFC of each group is represented graphically in Figure 7 and the average scores received for each scoring parameter are tabulated in Supplementary Figure 3. All of the groups had a total score of close to 20 (out of 28), with higher SDs observed in both of the groups where gradient scaffolds were soaked with growth factors. There were no statistically significant differences in the total histological scores among the groups.

The gradient scaffold-only group had lacunated cells with morphology that resembled cells of the hyaline cartilage and had normal to moderate levels of Saf-O staining. The cells appeared in isogenic groups and had a columnar arrangement in the proliferative zone. Cell clustering was observed in <25% of the total cells, mostly toward the deep or hypertrophic zone of the cartilage. The cartilage had slight disintegration, including cysts, with near to normal integrity as that of native cartilage. The degenerative changes on the surrounding cartilage was scored and had an average score of greater than 2, which indicated normal cellularity, mild clusters and moderate Saf-O staining. There was no inflammatory reaction in the subchondral bone.

Microfracture group condyles had an average score of 2.5 for Saf-O staining, which indicated near to normal Saf-O staining. This group also received a score of 2.5 for cellularity. Condyles that displayed multiple small fissures on the cartilage contained mostly fibrous chondrocytes or chondrocyte clusters in the resting and proliferative zones, which indicated signs of degeneration as shown in Supplementary Figures 4 & 5. Structural features were similar to native cartilage and exhibited normal cellularity, mild clusters and moderate Saf-O staining in the cartilage surrounding the defect.

The cells in the TGF-β3 group had mostly lacunated cells that resembled the morphology of cells in hyaline cartilage; the translucent cartilage in this group displayed either moderate or slight staining for Saf-O. The TGF-β3 group received the highest average score for structural integrity. The IGF group contained either a mixture of hyaline and fibrocartilage, or fibrocartilage alone. The cartilage was more opaque with a higher average score of 2.5 for Saf-O staining. In most of the samples in the TGF-β3 and

Table 1. MRI grading scale and average scores received for the lateral femoral condyles and medial femoral condyles of sheep 4 months post-implantation.

MRI grading criteria	Groups	MFC average	LFC average	General trend
Articular surface defect fill:				
– 0: No defect seen	Gradient scaffold	2.7 ± 1.5	2.3 ± 1.5	Higher articular surface filling was observed in MFC samples; TGF-β3 infiltrated scaffolds dominated lateral filling
– 1:0–25%	Gradient scaffold + TGF-β3	2.0 ± 1.7	3.7 ± 0.6†	
– 2: 26–50%	Gradient scaffold + IGF	1.7 ± 1.2	3.0 ± 1.0	
– 3: 51–75%	Microfracture	4.0 ± 0†	2.0 ± 1.0	
– 4: 76–100%				
Subchondral trabecular bone defect fill:				
– 0: No defect seen	Gradient scaffold	1.3 ± 0.6	1.3 ± 0.6	Microfracture showed better defect fill in the bone due to small holes in the subchondral bone
– 1:0–25%	Gradient scaffold + TGF-β3	2.0 ± 1.0	2.0 ± 1.0	
– 2: 26–50%	Gradient scaffold + IGF	2.0 ± 1.0	2.6 ± 1.2	
– 3: 51–75%	Microfracture	3.0 ± 1.0†	3.0 ± 0†	
– 4: 76–100% fill				
Subchondral trabecular bone sclerosis:				
– 0: None	Gradient scaffold	2.0 ± 2†	2.0 ± 1†	Highest sclerosis was observed for microfracture group in MFC
– 1: Slight	Gradient scaffold + TGF-β3	2.7 ± 2.3	3.0 ± 0	
– 2: Mild	Gradient scaffold + IGF	3.7 ± 0.6	2.3 ± 0.6	
– 3: Moderate	Microfracture	4.0 ± 0	3.0 ± 0	
– 4: Severe				
Subchondral trabecular bone edema:				
– 0: None	Gradient scaffold	2.7 ± 2.3	0†	Moderate edema was observed in MFC. Negligible level of edema was observed in LFC
– 1: Slight	Gradient scaffold + TGF-β3	2.7 ± 2.3	0.3 ± 0.6	
– 2: Mild	Gradient scaffold + IGF	2.3 ± 2.1†	0.3 ± 0.6	
– 3: Moderate	Microfracture	3.3 ± 0.6	1.3 ± 1.5	
– 4: Severe				
Joint effusion:				
– 0: None	Gradient scaffold	2.7 ± 0.6		Moderate-to-severe joint effusion was observed in Gradient scaffold and the TGF-β infiltrated samples

Average scores were represented as means ± standard deviations (n = 3).
†Highest favorable score.
LFC: Lateral femoral condyle; MFC: Medial femoral condyle.

Table 1. MRI grading scale and average scores received for the lateral femoral condyles and medial femoral condyles of sheep 4 months post-implantation (cont.).

MRI grading criteria	Groups	MFC average	LFC average	General trend
Joint effusion (cont.):				
– 1: Mild	Gradient scaffold + TGF-β3	2.3 ± 1.2		
– 2: Moderate	Gradient scaffold + IGF	1.0 ± 0†		
– 3: Severe	Microfracture	1.3 ± 1.2		
Synovitis:				
– 0: None	Gradient scaffold	0.3 ± 0.6†		Mild synovitis were present in few samples in all of the groups
– 1: Present	Gradient scaffold + TGF-β3	0.6 ± 0.6		
	Gradient scaffold + IGF	0.3 ± 0.6†		
	Microfracture	0.3 ± 0.6†		
Joint capsule thickening:				
– 0: None	Gradient scaffold	0.6 ± 0.6		No capsule thickening was observed in the joint in the IGF infiltrated and the microfracture group
– 1: Present	Gradient scaffold + TGF-β3	0.3 ± 0.6		
	Gradient scaffold + IGF	0†		
	Microfracture	0†		

Average scores were represented as means ± standard deviations (n = 3).
†Highest favorable score.
LFC: Lateral femoral condyle; MFC: Medial femoral condyle.

IGF pilot groups, cells appeared in isogenic groups and exhibited a columnar arrangement in the proliferative zone. Cell clustering was observed in <25% of the total cells mostly toward the deep or hypertrophic zones of the cartilage. The cartilage had either slightly higher than normal or close to normal thickness. There was slight disintegration, including cysts with near to normal integrity. Both the TGF-β3 and IGF groups had an average score of greater than 2 for degenerative changes in the surrounding cartilage, which indicated normal cellularity, mild clusters and moderate Saf-O staining, and either mild or no inflammatory reaction in the subchondral bone. Representative Sudan black staining of group I samples is represented in Supplementary Figure 6**.** Sudan black staining did not show any residual scaffold in the cartilage or in the subchondral bone for any individual sheep.

Discussion

The current study was the first to evaluate gradient scaffolds for cartilage repair in a long-term (1 year), large animal model, which was done with the clinical standard of care (i.e., microfracture) as a control to place the results of this first effort in context. In 2013, a review by Anderson *et al.* [34] stated that though there were several reports on the use of stem cells for cartilage repair in animals, both by direct injection and delivery using scaffolds, there was limited evidence of direct clinical benefit from the stem cells. Appropriate signals and microenvironment are required for tissue-specific osteochondral differentiation of progenitor cells. Hence, the current study investigated the potential of implanting gradient scaffolds engineered to recruit stem cells from the bone marrow into large defects for the purpose of regenerating bone and cartilage. We have previously investigated the potential of the microsphere-based scaffolds with gradients of growth factors, raw materials and combinations for both osteochondral tissue engineering *in vitro* and osteochondral regeneration *in vivo* in rabbits [10,20,35–36]. This is our first report on the long-term outcome of the implant of these gradient scaffolds in critical size osteochondral defects (6 mm diameter × 6 mm depth) in a large animal model.

In our previous studies, we encapsulated growth factors within the microspheres for controlled delivery [37–39]. As a translational study, growth factors were intentionally not encapsulated within the microspheres

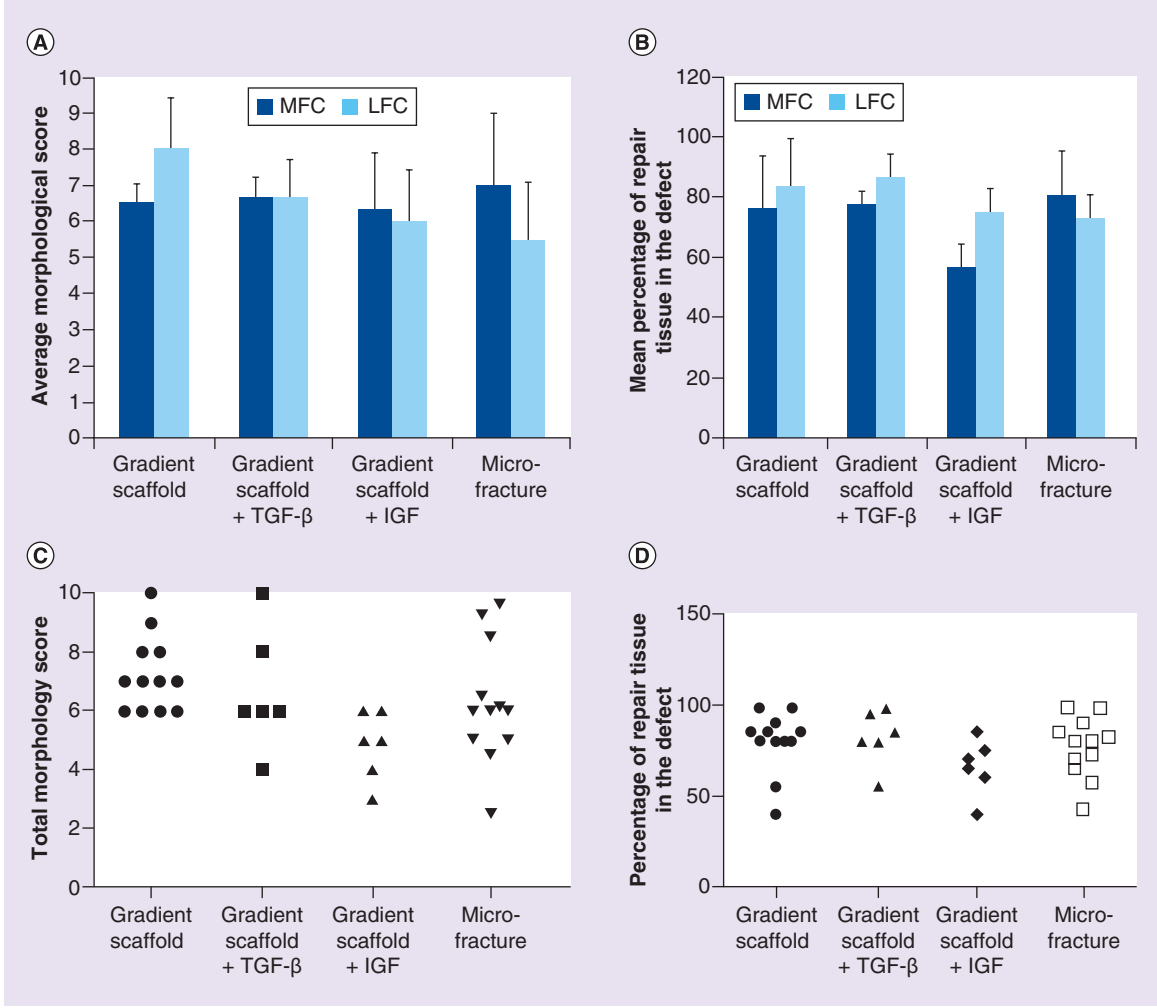

Figure 3. Gross morphological assessment of retrieved joints 1 year post-implantation. (A) The average morphological score in MFCs and LFCs, **(B)** the percentage of the repair tissue filled at the defect site in MFCs and LFCs, **(C)** the dot plot showing total morphological score distribution in each group and **(D)** the dot plot showing percentage of repair tissue fill in the defect in each group. Three independent co-authors compiled morphological scores based on parameters in Box 2. Average scores are represented as means ± standard deviations. The maximum possible score a healthy cartilage can receive is 10. Sample sizes are as follows: gradient only scaffold (n = 6), gradient scaffold + TGF-β3 (n = 3), gradient scaffold + IGF-1 (n = 3) and microfracture (n = 6). There were no statistically significant differences among the groups ($p > 0.05$).
LFC: Lateral femoral condyle; MFC: Medial femoral condyle.

in the current study, as to avoid US FDA designation as a combination drug product, although this upgrade can be made in the future to create further product separation in a competitive market. Instead, a 'raw materials' approach was taken whereby natural materials are leveraged both as building blocks to be incorporated into regenerating tissue and as signaling molecules to elicit desirable responses from infiltrating cells [40]. Our previous studies have demonstrated favorable cell responses to chondroitin sulfate [20,41–42], and β-TCP is a well-known building block for bone regeneration, which is more easily integrated into regenerating bone than the hydroxyapatite we have used in our previous microsphere-based scaffold studies [10,35,43].

In addition, pilot groups including specific doses of either the chondrogenic signal TGF-β3 or the anabolic signal IGF-1 were added in a drop-wise manner to the gradient plugs immediately prior to implantation in the operating room. Previous reports indicate TGF-β3 is more responsive than TGF-β1 for chondrogenesis. Rat mesenchymal stem cells seeded on 3D porous semi IPN scaffold secreted significantly higher amount of total GAG and collagen content and had more collagen type II when supplemented with TGF-β3 than TGF-β1 [44]. Our previous report on TGF-β3-chondroitin sulfate combination encapsulated in PLGA microspheres was found to favor chondrogenic differentiation of stem cells [20]. The rationale for these pilot

groups was that if any given osteochondral implant product were to be approved without growth factors, then an orthopedic surgeon would have the discretion of whether to add a given dose of a given growth factor to the plug immediately before implantation. The administration route was selected as a new approach for biomaterials in cartilage regeneration. If a material alone is sufficient for FDA approval as a device, and if the medical literature were to show that addition of a metered dose of growth factor by the surgeon in the operating room to the material were to be even more effective, then although the company could not market their product as such, surgeons may have a basis for achieving superior regeneration by combining two distinct, separate products. This may also provide biological activity superior to that with encapsulation [45,46].

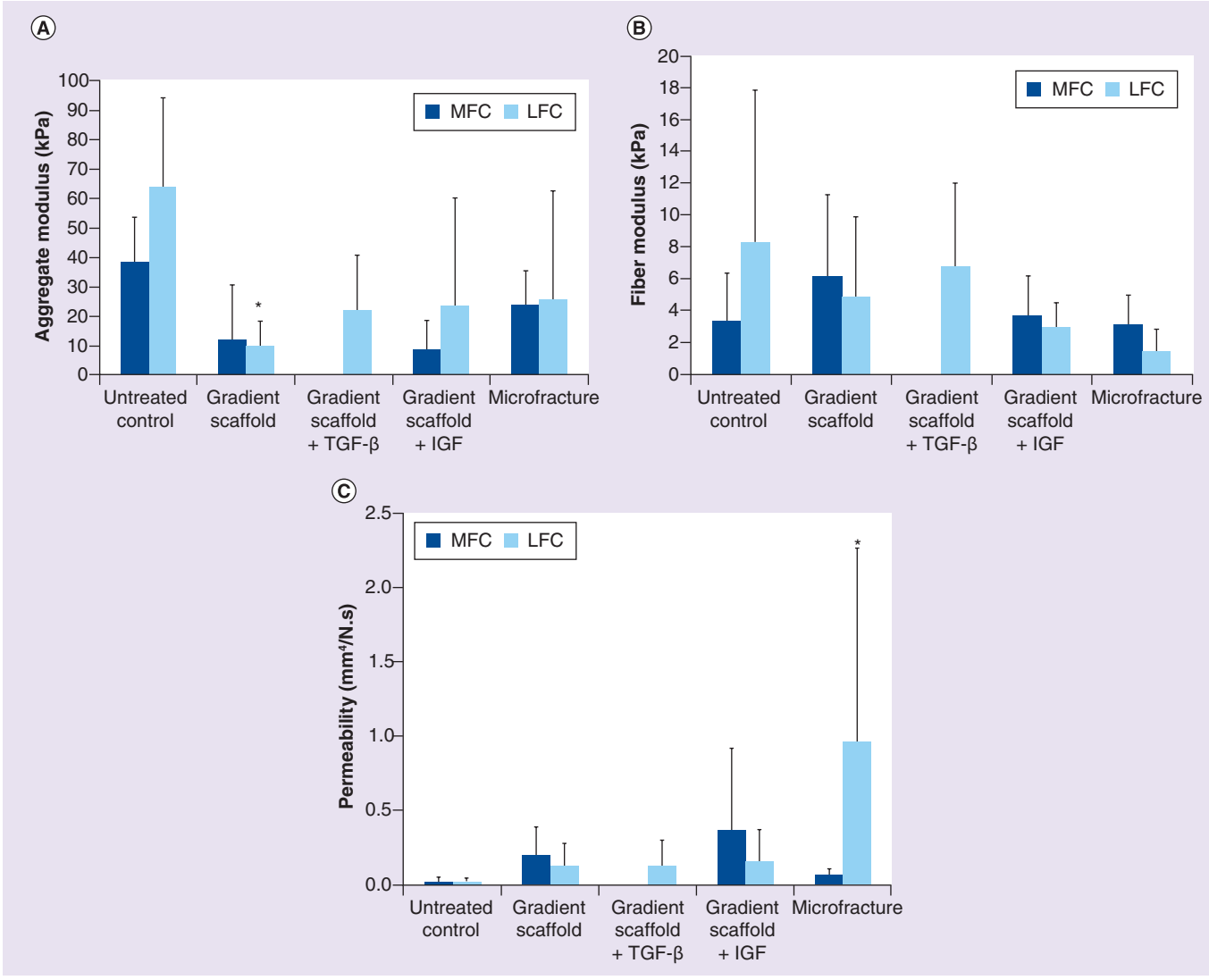

Figure 4. Mechanical testing of repair tissue in retrieved joints 1 year post-implantation. (A) the aggregate modulus, **(B)** fiber modulus and **(C)** permeability of regenerated tissue. Joints retrieved 1 year post-implantation were subjected to uniaxial compressive indentation and modeled with the biphasic theory, with the solid phase consisting of a biphasic material with a 'neo-Hookean' ground matrix and a spherical fiber distribution to model the collagen fibrillar matrix [33]. Note that the LFC of the microfracture group had the only permeability to be statistically significantly larger than the untreated control, whereas the gradient LFC group had the only aggregate modulus statistically significantly below that of the untreated control. Although the MFC of the TGF group qualitatively appeared to be stiffer than the other groups, the fit to the model was insufficient to allow us to report the data. Taken together, these data are not able to confirm a clear difference between the gradient groups and the microfracture group. Use of a spherical indenter in the future may allow us to achieve tighter standard deviations. Average scores were represented as means ± standard deviations. Sample sizes were as follows: gradient scaffold (n = 6), gradient scaffold + TGF-β3 (n = 3), gradient scaffold + IGF (n = 3) and microfracture (n = 6).
*Represents significant difference from untreated control ($p < 0.05$).
LFC: Lateral femoral condyle; MFC: Medial femoral condyle.

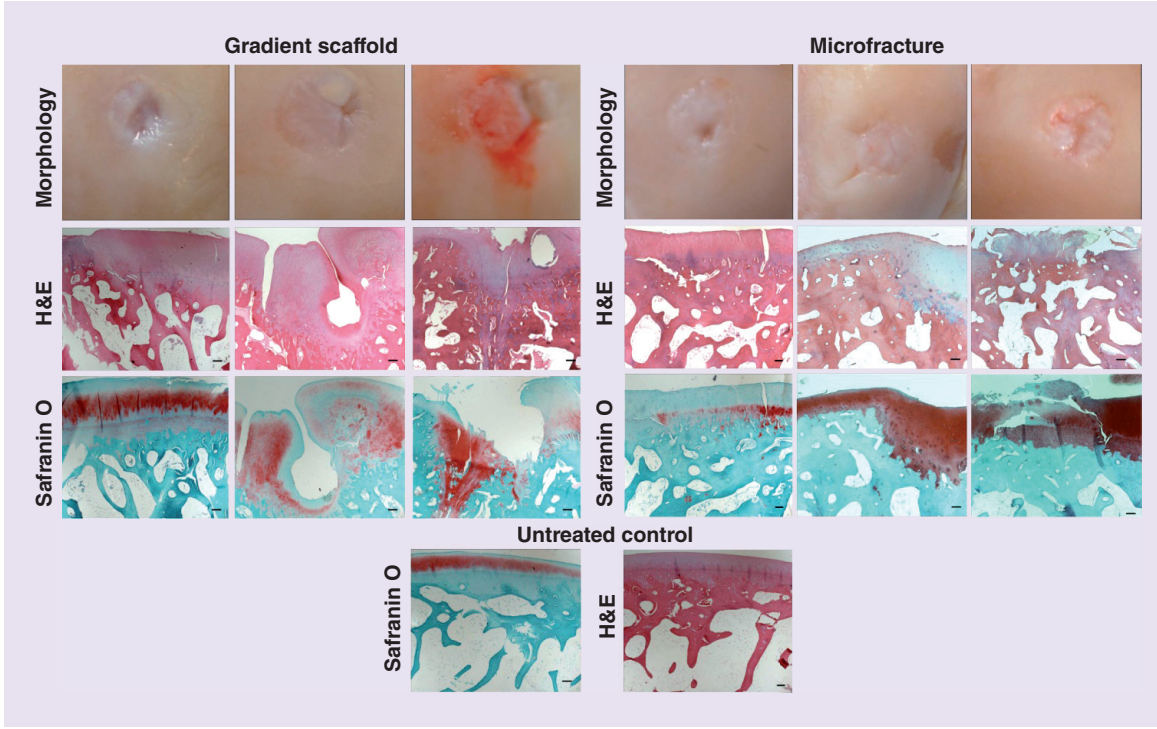

Figure 5. Representative images for gross morphology and histological analysis of the gradient scaffold-only group and the microfracture group at 1 year post-implantation. Each column in the left panel represents a representative sample that received high (D01 medial femoral condyle [MFC]: score 24), medium (D02 MFC: score 20) and low (D04 MFC: score 13) histological scores of for the gradient scaffold-only group. Total scores for the gradient scaffold-only group were in the range of 13–26 (out of 28). Each column in the right panel represents a representative sample that received high (D15 lateral femoral condyle [LFC] score 25), medium (D16 LFC: score 21) and low (D17 LFC: score 18) histological scores in the microfracture group. Total scores for microfracture group were in the range of 15 to 25. The cells in gradient scaffold-only group had lacunated cells and resembled those normally seen in hyaline cartilage, and normal to moderate levels of Safranin-O staining and had no inflammatory reaction in the subchondral bone. The microfracture group had near to normal Safranin-O staining, had cells resemble those normally seen in hyaline cartilage or fibrous chondrocytes and chondrocyte clusters in the resting and proliferative zone, which indicated signs of degeneration. The bottom row represents images of untreated control. H&E and Safranin O staining shows the cellular morphology and glycosaminoglycan deposition respectively. The scale bars: 200 μm.
H&E: Hematoxylin & Eosin.

These groups were intended merely as a demonstration of feasibility and proof of concept, with full appreciation for and recognition of the need for larger dose-response studies in the future to enable surgeons to make evidence-based decisions in the operating room.

Our results indicated that although 50% of TGF-β3 infiltrated scaffolds generated a translucent cartilage similar to hyaline cartilage, which appeared smooth and covered most of the defect site; the other 50% of condyles had either a rough surface or fibrous outgrowth and had a higher SD in the histological score. Moreover, within this TGF group, signs of osteoarthritis in patella and infections in marrow were observed in two sheep during necropsy. Therefore, disorders not related to the implant might have also influenced the regeneration of cartilage in of this group, or *vice versa*. The IGF-1 infiltrated scaffolds failed to regenerate the cartilage completely and had fissures at the edges or at the center. The amount of IGF-1 used in this study was lower than what was reported in the literature for *in vivo* applications in horses [21–22,47]. The suitability of the growth factor absorbed implantation procedure for gradient scaffolds could not be effectively established in this study due to the smaller sample sizes. A few of the gradient scaffolds treated with TGF-β3 appeared to be beneficial, which warrants further investigation into use of TGF-β3 either via dropwise addition in the operating room, or by encapsulation for future generations of this technology. In the gradient scaffolds treated with IGF-1, the dose or the route of administration of IGF-1 (not encapsulating) require further optimization.

The MRI data collected at 4 months after implantation indicated that bone regeneration was less in the gradient scaffold groups compared with the microfracture group. This was because the gradient scaffold

groups had osteochondral defects, whereas the microfracture group only received a chondral (shallower) defect. Moreover, the PLGA used for the osteogenic microspheres in gradient scaffolds were tailored to degrade slower so as to provide structural support for a longer period of time. Hence, remnants of the scaffold were visible in the MRI 4 months after implantation. Though at a slower degradation rate, the osteogenic microspheres appeared to be sufficient to maintain structure, although it is possible that it may have been an obstacle in the way of the regenerating tissue, and future studies are warranted to fine tune the parameter of degradation rate in gradient scaffold received animals.

In hindsight, we believe that a defect depth of 6 mm may have been too deep for the implant groups, creating more damage than necessary to achieve the objective of providing a source of MSCs and osseous integration for the implants. A slightly shallower defect may be beneficial for creating the osteochondral defect to leverage the infiltration of MSCs and integration with the bone for future studies, perhaps accelerating regeneration and leading to better long-term cartilage regeneration.

To compare the primary test group (i.e., gradient only) to the standard-of-care control (i.e., microfracture), the regeneration in the group that received gradient scaffolds alone surpassed the microfracture group in terms of structure and appearance. The cartilage of the gradient scaffold-only group was mostly translucent and smooth and the gross morphology more resembled the native cartilage in appearance. The defect was covered in most of the samples and only a fourth of the samples showed a fissure either at the center or at the edge of the defect. On the contrary, the repair tissues in the microfracture group were mostly opaque and more than 50% of the samples had scattered fissures or multiple smaller cracks on the surface. The total morphological score for all of the condyles in the gradient scaffold-only group were in the range of 6–10. The tissue fill in this group was >80% in all but one animal. In contrast, there was a wider distribution in total morphological scores and in percentage repair tissue fill in the microfracture group. The morphological scores for the microfracture group were distributed in the wide range of 2.5–9.6 with 100% of the sheep having a score <6 in either the left or right condyle. Approximately 50% of the animals had <80% tissue fill on both of the condyles in the microfracture group. Overall, our analyses indicated that gradient scaffolds outperformed

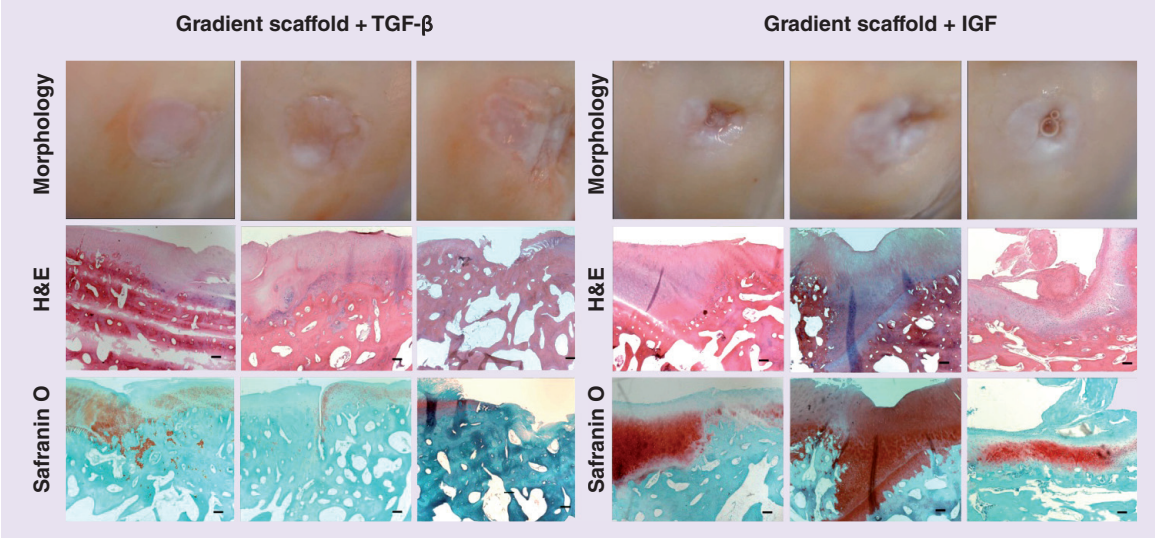

Figure 6. Representative images for gross morphology and histological analysis of the gradient scaffold + TGF-β and the gradient scaffold + IGF at 1 year post-implantation. Each column in the left panel represents a representative sample that received high (D08 medial femoral condyle [MFC]: score 22), medium (D08 lateral femoral condyle [LFC]: score 21) and low (D07 MFC: 7) histological scores for the gradient scaffold + TGF-β group. Total scores for the gradient scaffold + TGF-β group were in the range of 7 to 22. Each column in the right panel represents a representative sample that received high (D12 MFC: score 27), medium (D11 MFC: score 23) and low (D11 LFC: score 12) histological scores of the gradient scaffold + IGF group. Total scores for gradient scaffold + IGF were in the range of 12 to 27. The cells in gradient scaffold treated with TGF-β3 group had mostly lacunated cells that resembled those normally seen in hyaline cartilage; the translucent cartilage in this group displayed either moderate or slight staining for Safranin-O. Gradient scaffold treated with IGF-1 group contained either a mixture of hyaline and fibrocartilage, or fibrocartilage alone. The cartilage was more opaque with moderate to nearly normal Safranin-O staining. Scale bars: 200 μm.
H&E: Hematoxylin & Eosin.

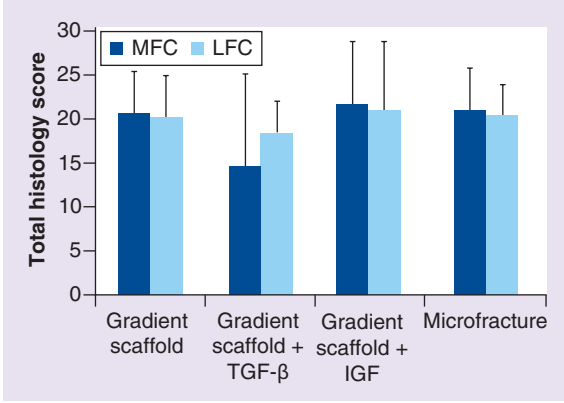

Figure 7. Total histology scores received for each groups. Joints retrieved 1 year post-implantation were stained with Hematoxylin & Eosin and Safranin-O and scored using a modified O'Driscoll score [30]. Histology scores were compiled by three co-authors based on parameters in Box 3. The maximum possible score is 28. Average scores are represented as means ± standard deviation. Gradient scaffold only group (n = 6), gradient scaffold + TGF-β3 group (n = 3), gradient scaffold + IGF group (n = 3) and microfracture group (n = 6). There were no statistically significant differences among the groups ($p > 0.05$).
LFC: Lateral femoral condyle; MFC: Medial femoral condyle.

microfracture in forming a smoother regenerated tissue without cracks.

The results of the microfracture group are consistent with previous reports on the performance of the microfracture technique, which have also indicated that defects treated with microfracture heal via formation of a repair tissue that filled in the microfracture 'holes' and 'crept' over the surface of the defect, forming islands of cartilage that deteriorated with mechanical loading in the long term [48]. Though microfracture is the 'gold standard treatment' for repairing cartilage defects, microfracture has been reported to form granulation tissue that is replaced by fibrocartilage and eventually fibrous tissue [2].

It has been reported that the fibrous tissue of microfracture, while filling the defect, is inferior in mechanical performance when compared with hyaline cartilage, and fibrous tissue often degenerates with mechanical loading and deteriorates following microfracture after 2 years [49]. In osteoarthritic cartilage, an increase in permeability is attributed to a decrease in proteoglycan content that creates more space in the matrix, resulting in lower compressive stiffness and rapid deformation. The permeability of the tissue in the microfracture groups in the LFC was 45-times higher than the control native joint; however, uniform deposition of glycosaminoglycan (GAG) was present in the regenerated cartilage of most of the animals of this group; therefore the increase in permeability could not be directly attributed to lower GAG content, but perhaps instead due to the structure of the tissue (e.g., formation of large aggrecan molecules). Deformation-dependent permeability is a valuable mechanism for load sharing between the solid phase and the fluid phase of the cartilage [50]. When the fluid flows easily out of the tissue due to high permeability, then the solid matrix bears the full contact stress, and under this increased stress, the tissue is more prone to failure. Hence, the formation of multiple cracks in the cartilage of the microfracture group may be the cause of higher permeability. The permeability was lower and comparable to native cartilage in the MFC of the microfracture group and an increase in aggregate modulus was also observed.

The histology observations indicated that there were no significant differences in the total histology scores among the groups. It should be noted that the histology data showed a general trend of regeneration associated with each group; however, the trend was not exactly uniform in all of the sections, as these are representative sections taken from the entire defect area of the regenerated cartilage. The cells resembled those normally seen in hyaline cartilage in the gradient scaffold-only group and in the TGF-β3 group. Cell clusters were observed toward the hypertrophic region in most of the gradient scaffold-only including TGF and IGF condyles; however, chondrocyte clusters indicating signs of degenerative cartilage were observed in all of the samples that had multiple fissures in the microfracture group. All of the gradient scaffold-only samples including TGF and IGF samples had favorable scores for cellular features with fewer degenerative changes and uniform performance from sample to sample, whereas microfracture samples had higher variation. More information about cell performance would be of interest and detailed cell analysis such as *in situ* hybridization may be of value in the future. The defect site in the gradient scaffold-only, did not show any inflammatory response, which indicated that neither the byproducts of degraded scaffolds nor the raw materials released into the defect area induced any toxic response. The GAG deposition was slightly lesser in the TGF-β3 group.

Now that measurable and observable differences have been established between the ability of using a gradient scaffold to regenerate cartilage versus the technique of microfracture, there is motivation and a strong rationale for refining the gradient scaffolds (e.g., PLGA degradation rate, raw material dose) for further testing in preclinical studies. Furthermore, follow-up experiments that investigate gradient scaffold incubation with other growth factors or combinations of growth factors will yield valuable information regarding regeneration and remodeling time for cartilage formation. More detailed analysis regarding inflammation and cellular response

will additionally provide beneficial data for further enhancing the use of gradient biomaterials in regenerative applications.

Conclusion

The current standard of care for cartilage repair in the knee is microfracture, where a full-thickness chondral-only defect is treated via, small holes created through the subchondral bone plate to release marrow cells into the defect. Microfracture is limited in its ability to regenerate hyaline cartilage, and patients are not able to return to normal weight-bearing activity for several weeks. The current study made a direct comparison between two different approaches to cartilage repair: microfracture (standard of care control), and an osteochondral approach with microsphere-based gradient plugs. We engineered osteochondral scaffolds with continuous opposing gradients of 'raw materials', CS and β-TCP, to implant into critical size defects of the right knee joint of sheep for the purpose of evaluating cartilage regeneration with gradient scaffolds against microfracture. Furthermore, we demonstrated that metered doses of either TGF-β3 or IGF-1 could be added to the gradient scaffolds in the operating room immediately prior to implantation. The current study is the first to evaluate gradient scaffolds in a large animal model, and demonstrated that CS/β-TCP gradient scaffolds regenerated cartilage that was more native-like (hyaline cartilage) in terms of structure, gross appearance and cell morphology than the fibrous tissue that forms as a result of microfracture, even in spite of regenerating deeper osteochondral defects compared with the shallower chondral-only defects with microfracture. The current study has established proof of concept and feasibility with a large animal model. The microsphere-based gradient plugs in the clinic may hold the additional advantage of rapid return to weight-bearing activity.

Future perspective

The major clinical challenge for cartilage repair in the knee is that hyaline articular cartilage regeneration both at the structural and functional/mechanical levels has not been achieved in adults using microfracture technique, the current standard of care [51]. Further in the microfracture approach, there is no possibility to directly control the chondrogenic process, which may depend on a number of local as well as systemic factors that can be patient-specific [52]. A better control of chondrogenesis might be achieved by supplementing microfracture procedure with a multifaceted scaffold, an intelligent biomaterial possibly supplemented with biological factors to control and enhance repair [53]. It is known that the quality of cartilage regenerated in an empty osteochondral defects is of poor quality. Previous reports indicate that in empty osteochondral control defects neither bone nor cartilage is formed; the repair tissue formed is fibrous or a mixed-type fibrocartilage tissue with poor integration with the surrounding cartilage [44,54–55]. In our study we used a gradient 3D osteochondral scaffold that encapsulated raw materials, chondrodroitin sulfate and β tricalcium phosphate. Recruiting autologous progenitor cells from bone marrow toward the scaffold facilitated simultaneous regeneration of both cartilage and a stable bone [10]. The current study in critical size defect in large animal regenerated cartilage that was more native-like (hyaline cartilage) in terms of structure, gross appearance and cell morphology and stable matrix as opposed to the fibrous tissue with fissures and degenerative changes in microfracture. Immunostaining for collagen did not provide reliable and consistent information with the histological processing method used, and was thus not included and is a limitation of the current study.

Future studies can explore the use of osteochondral defects that are less deep, better matching the scaffold and drill bit dimensions, refining scaffold parameters including PLGA degradation rate and raw material concentration. An obvious advantage of the pilot growth factor groups could not be demonstrated in the current study. Further, we plan to optimize dosing of growth factor or go for growth factor encapsulation to determine whether a greater extent of superiority over microfracture could be attained in a preclinical model and to carry out large animal studies with statistically significant number of animals.

Acknowledgements

M Barrett and A Valdes from Colorado State University are acknowledged for MRI analysis. G Ateshian from Columbia University is acknowledged for his generous guidance in the analysis of compression indentation data and assistance with FEBio software (www.febio.org).

Disclaimer

The content is solely the responsibility of the authors and does not necessarily represent the official views of the NIH.

Financial & competing interests disclosure

The authors gratefully acknowledge funding by the Coulter Foundation. In addition, this publication was supported by the National Institute of Arthritis and Musculoskeletal and Skin Diseases of the NIH under Award Number R01 AR056347. The authors would also like to recognize support from the Kansas Bioscience Authority Rising Star Award. The authors have no other relevant affiliations or financial involvement with any

organization or entity with a financial interest in or financial conflict with the subject matter or materials discussed in the manuscript apart from those disclosed.

No writing assistance was utilized in the production of this manuscript.

Ethical conduct of research

The authors state that they have obtained appropriate institutional review board approval or have followed the principles outlined in the Declaration of Helsinki for all human or animal experimental investigations. In addition, for investigations involving human subjects, informed consent has been obtained from the participants involved.

Supplementary data

To view the supplementary data that accompany this paper please visit the journal website at: www.futuremedicine.com/doi/full/10.2217/rme.15.38

Executive summary

Objective

- A direct comparison between microfracture (chondral-only repair) and an osteochondral approach with microsphere-based gradient plugs were made for cartilage repair for a period of one year in critical size defect in sheep (n = 6).

Methods

- Gradient scaffolds were composed of poly(lactic-*co*-glycolic acid) microspheres with opposing continuous gradients of chondroitin sulfate and β-tricalcium phosphate.
- In addition to the microfracture and gradient plugs, a pilot study was conducted in parallel, in critical size defect in sheep (n = 3) for 1 year, where precise quantities of either TGF-β3 or IGF-1 was added dropwise to gradient plugs prior to implantation.

Results

- The MRI data collected at 4 months after implantation, indicated that bone regeneration was less in the gradient scaffold groups (that received osteochondral defects) compared with the microfracture group (that received shallower chondral defects).
- Sheep that received gradient scaffolds regenerated cartilage, that was more native-like (hyaline cartilage) in terms of structure, gross appearance and cell morphology with equal or superior mechanical properties and had stable matrix with lesser degenerative changes
- Fibrous tissue was formed on microfracture group were cartilage was mostly opaque and had scattered fissures on the surface
- The obvious advantage of the pilot growth factor groups could not be demonstrated in the current study due to less sample number.

References

Papers of special note have been highlighted as:
•• of considerable interest

1 Brittberg M, Lindahl A, Nilsson A, Ohlsson C, Isaksson O, Peterson L. Treatment of deep cartilage defects in the knee with autologous chondrocyte transplantation. *N. Engl. J. Med.* 331(14), 889–895 (1994).

2 Breinan HA, Martin SD, Hsu HP, Spector M. Healing of canine articular cartilage defects treated with microfracture, a type-II collagen matrix, or cultured autologous chondrocytes. *J. Orthop. Res.* 18(5), 781–789 (2000).

3 Williams RJ 3rd, Harnly HW. Microfracture: indications, technique, and results. *Instr. Course Lect.* 56, 419–428 (2007).

4 Marquass B, Schulz R, Hepp P *et al.* Matrix-associated implantation of predifferentiated mesenchymal stem cells versus articular chondrocytes: *in vivo* results of cartilage repair after 1 year. *Am. J. Sports Med.* 39(7), 1401–1412 (2011).

5 Bentley G, Biant LC, Carrington RW *et al.* A prospective, randomised comparison of autologous chondrocyte implantation versus mosaicplasty for osteochondral defects in the knee. *J. Bone Joint Surg. Br.* 85(2), 223–230 (2003).

6 Laprade RF, Botker JC. Donor-site morbidity after osteochondral autograft transfer procedures. *Arthroscopy* 20(7), e69–e73 (2004).

7 Chiang H, Liao CJ, Hsieh CH, Shen CY, Huang YY, Jiang CC. Clinical feasibility of a novel biphasic osteochondral composite for matrix-associated autologous chondrocyte implantation. *Osteoarthr. Cartil.* 21(4), 589–598 (2013).

8 Jiang CC, Chiang H, Liao CJ *et al.* Repair of porcine articular cartilage defect with a biphasic osteochondral composite. *J. Orthop. Res.* 25(10), 1277–1290 (2007).

9 Shimomura K, Moriguchi Y, Murawski CD, Yoshikawa H, Nakamura N. Osteochondral tissue engineering with biphasic scaffold: current strategies and techniques. *Tissue Eng. B Rev.* 20(5), 468–476 (2014).

10 Mohan N, Dormer NH, Caldwell KL, Key VH, Berkland CJ, Detamore MS. Continuous gradients of material composition and growth factors for effective regeneration of the osteochondral interface. *Tissue Eng. A* 17(21–22), 2845–2855 (2011).

•• **Demonstrates *in vivo* that microsphere based scaffolds with material and growth factor gradients enabled formation of a stable cartilage layer with proper integration with the**

surrounding cartilage and underlying bone in critical size defects in rabbit knee joints.

11 Agrawal CM, Athanasiou KA. Technique to control pH in vicinity of biodegrading PLA-PGA implants. *J. Biomed. Mater. Res.* 38(2), 105–114 (1997).

12 Singh M, Dormer N, Salash JR *et al.* Three-dimensional macroscopic scaffolds with a gradient in stiffness for functional regeneration of interfacial tissues. *J. Biomed. Mater. Res. A* 94(3), 870–876 (2010).

13 Singh M, Morris CP, Ellis RJ, Detamore MS, Berkland C. Microsphere-based seamless scaffolds containing macroscopic gradients of encapsulated factors for tissue engineering. *Tissue Eng. Part C Methods* 14(4), 299–309 (2008).

•• **Demonstrates the fabrication of monodisperse microspheres and 3D microsphere based gradient scaffold for tissue engineering and drug delivery applications.**

14 Dormer NH, Singh M, Wang L, Berkland CJ, Detamore MS. Osteochondral interface tissue engineering using macroscopic gradients of bioactive signals. *Ann. Biomed. Eng.* 38(6), 2167–2182 (2010).

•• **Demonstrates that human bone marrow and umbilical cord mesenchymal stromal cells produced regionalized extracellular matrix in response to gradients of TGFβ-3 and BMP-2 in microsphere-based 3D scaffoldss. The study proved that engineered signal gradients may be beneficial for osteochondral tissue engineering.**

15 Singh M, Berkland C, Detamore MS. Strategies and applications for incorporating physical and chemical signal gradients in tissue engineering. *Tissue Eng. B Rev.* 14(4), 341–366 (2008).

16 Borden M, Attawia M, Khan Y, El-Amin SF, Laurencin CT. Tissue-engineered bone formation *in vivo* using a novel sintered polymeric microsphere matrix. *J. Bone Joint Surg. Br.* 86(8), 1200–1208 (2004).

17 Bhamidipati M, Scurto AM, Detamore MS. The future of carbon dioxide for polymer processing in tissue engineering. *Tissue Eng. B Rev.* 19(3), 221–232 (2013).

18 Jeon JH, Bhamidipati M, Sridharan B, Scurto AM, Berkland CJ, Detamore MS. Tailoring of processing parameters for sintering microsphere-based scaffolds with dense-phase carbon dioxide. *J. Biomed. Mater. Res. B Appl. Biomater.* 101(2), 330–337 (2013).

19 Schagemann JC, Erggelet C, Chung HW, Lahm A, Kurz H, Mrosek EH. Cell-laden and cell-free biopolymer hydrogel for the treatment of osteochondral defects in a sheep model. *Tissue Eng. Part A* 15(1), 75–82 (2009).

20 Mohan N, Gupta V, Sridharan B, Sutherland A, Detamore MS. The potential of encapsulating "raw materials" in 3D osteochondral gradient scaffolds. *Biotechnol. Bioeng.* 111(4), 829–841 (2014).

•• **Demonstrates that the raw materials encapsulated in 3D gradient scaffolds produced clear regional variations in the secretion of tissue-specific ECM. They created a favorable microenvironment for cells and can significantly enhance the synthesis of certain extracellular matrix components. Success with raw materials in lieu of growth factors could have profound implications in terms of lower cost and faster regulatory approval for more rapid translation of regenerative medicine products to the clinic.**

21 Schmidt M, Chen E, Lynch S. A review of the effects of insulin-like growth factor and platelet derived growth factor on *in vivo* cartilage healing and repair. *Osteoarthritis Cartilage* 14(5), 403–412 (2006).

22 Fortier LA, Mohammed HO, Lust G, Nixon AJ. Insulin-like growth factor-I enhances cell-based repair of articular cartilage. *J. Bone Joint Surg. Br.* 84(2), 276–288 (2002).

23 Athanasiou KA, Rosenwasser MP, Buckwalter JA, Malinin TI, Mow VC. Interspecies comparisons of *in situ* intrinsic mechanical properties of distal femoral cartilage. *J. Orthop. Res.* 9(3), 330–340 (2005).

24 Kim K-W, Wong ME, Helfrick JF, Thomas JB, Athanasiou KA. Biomechanical tissue characterization of the superior joint space of the porcine temporomandibular joint. *Ann. Biomed. Eng.* 31(8), 924–930 (2003).

25 Mow VC, Kuei SC, Lai WM, Armstrong CG. Biphasic creep and stress relaxation of articular cartilage in compression? Theory and experiments. *J. Biomech. Eng.* 102(1), 73–84 (1980).

26 Bonet J, Wood RD. *Nonlinear Continuum Mechanics For Finite Element Analysis.* Cambridge University Press, Cambridge; New York, NY, USA (1997).

27 Huang AH, Baker BM, Ateshian GA, Mauck RL. Sliding contact loading enhances the tensile properties of mesenchymal stem cell-seeded hydrogels. *Eur. Cell Mater.* 24, 29–45 (2012).

28 Ateshian GA, Rajan V, Chahine NO, Canal CE, Hung CT. Modeling the matrix of articular cartilage using a continuous fiber angular distribution predicts many observed phenomena. *J. Biomech. Eng.* 131(6), 061003 (2009).

29 FEBio. www.febio.org

30 Frisbie DD, Bowman SM, Colhoun HA, Dicarlo EF, Kawcak CE, Mcilwraith CW. Evaluation of autologous chondrocyte transplantation via a collagen membrane in equine articular defects: results at 12 and 18 months. *Osteoarthritis Cartilage* 16(6), 667–679 (2008).

31 O'driscoll SW, Keeley FW, Salter RB. The chondrogenic potential of free autogenous periosteal grafts for biological resurfacing of major full-thickness defects in joint surfaces under the influence of continuous passive motion. An experimental investigation in the rabbit. *J. Bone Joint Surg. Am.* 68(7), 1017–1035 (1986).

32 O'driscoll SW, Keeley FW, Salter RB. Durability of regenerated articular cartilage produced by free autogenous periosteal grafts in major full-thickness defects in joint surfaces under the influence of continuous passive motion. A follow-up report at one year. *J. Bone Joint Surg. Am.* 70(4), 595–606 (1988).

33 Ateshian GA, Rajan V, Chahine NO, Canal CE, Hung CT. Modeling the matrix of articular cartilage using a continuous fiber angular distribution predicts many observed phenomena. *J. Biomech. Eng.* 131(6), 061003 (2009).

34 Anderson JA, Little D, Toth AP *et al.* Stem Cell therapies for knee cartilage repair: the current status of preclinical and clinical studies. *Am. J. Sports Med.* 42(9), 2253–2261 (2013).

35 Dormer NH, Qiu Y, Lydick AM *et al.* Osteogenic differentiation of human bone marrow stromal cells in hydroxyapatite-loaded microsphere-based scaffolds. *Tissue Eng. Part A* 18(7–8), 757–767 (2012).

36 Dormer NH, Singh M, Zhao L, Mohan N, Berkland CJ, Detamore MS. Osteochondral interface regeneration of the rabbit knee with macroscopic gradients of bioactive signals. *J. Biomed. Mater. Res. A* 100(1), 162–170 (2012).

37 Park JS, Yang HJ, Woo DG, Yang HN, Na K, Park K-H. Chondrogenic differentiation of mesenchymal stem cells embedded in a scaffold by long-term release of TGF-β3 complexed with chondroitin sulfate. *J. Biomed. Mater. Res. Part A* 92(2), 806–816 (2009).

38 Hellingman CA, Davidson EN, Koevoet W *et al.* Smad signaling determines chondrogenic differentiation of bone-marrow-derived mesenchymal stem cells: inhibition of Smad1/5/8P prevents terminal differentiation and calcification. *Tissue Eng. Part A* 17(7–8), 1157–1167 (2011).

39 Almeida HV, Liu Y, Cunniffe GM *et al.* Controlled release of transforming growth factor-beta3 from cartilage-extra-cellular-matrix-derived scaffolds to promote chondrogenesis of human-joint-tissue-derived stem cells. *Acta Biomater.* 10(10), 4400–4409 (2014).

40 Renth AN, Detamore MS. Leveraging "raw materials" as building blocks and bioactive signals in regenerative medicine. *Tissue Eng. B Rev.* 18(5), 341–362 (2012).

41 Ingavle GC, Frei AW, Gehrke SH, Detamore MS. Incorporation of aggrecan in interpenetrating network hydrogels to improve cellular performance for cartilage tissue engineering. *Tissue Eng. Part A* 19(11–12), 1349–1359 (2013).

42 Ingavle GC, Dormer NH, Gehrke SH, Detamore MS. Using chondroitin sulfate to improve the viability and biosynthesis of chondrocytes encapsulated in interpenetrating network (IPN) hydrogels of agarose and poly(ethylene glycol) diacrylate. *J. Mater. Sci. Mater. Med.* 23(1), 157–170 (2012).

43 Dormer NH, Gupta V, Scurto AM, Berkland CJ, Detamore MS. Effect of different sintering methods on bioactivity and release of proteins from PLGA microspheres. *Mater. Sci. Eng. C. Mater. Biol. Appl.* 33(7), 4343–4351 (2013).

44 Mohan N, Nair PD, Tabata Y. Growth factor-mediated effects on chondrogenic differentiation of mesenchymal stem cells in 3D semi-IPN poly(vinyl alcohol)-poly(caprolactone) scaffolds. *J. Biomed. Mater. Res. A* 94(1), 146–159 (2010).

45 Lee K, Silva EA, Mooney DJ. Growth factor delivery-based tissue engineering: general approaches and a review of recent developments. *J. R. Soc. Interface* 8(55), 153–170 (2010).

46 Chen F-M, Zhang M, Wu Z-F. Toward delivery of multiple growth factors in tissue engineering. *Biomaterials* 31(24), 6279–6308 (2010).

47 Nixon AJ, Fortier LA, Williams J, Mohammed H. Enhanced repair of extensive articular defects by insulin-like growth factor-I-laden fibrin composites. *J. Orthop. Res.* 17(4), 475–487 (1999).

48 Power J, Hernandez P, Guehring H, Getgood A, Henson F. Intra-articular injection of rhFGF-18 improves the healing in microfracture treated chondral defects in an ovine model. *J. Orthop. Res.* 32(5), 669–676 (2014).

•• **Demonstrates that supplementing biological cues enhances cartilage repair in microfracture procedure.**

49 Mithoefer K, Williams RJ 3rd, Warren RF *et al.* The microfracture technique for the treatment of articular cartilage lesions in the knee. A prospective cohort study. *J. Bone Joint Surg. Am.* 87(9), 1911–1920 (2005).

50 Mansour JM. *Biomechanics of Cartilage.* Oatis CA (Ed.), Lippincott Williams & Wilkins, MD, USA, 1992–1996 (2003).

51 Madry H, Grun UW, Knutsen G. Cartilage repair and joint preservation: medical and surgical treatment options. *Dtsch Arztebl. Int.* 108(40), 669–677 (2011).

52 Cucchiarini M, Madry H, Guilak F *et al.* A vision on the future of articular cartilage repair. *Eur. Cell Mater.* 27, 12–16 (2014).

•• **Comments on the limitations of current standards of care for cartilage repair, suggests improvements on existiong sugical techniques and the need to use a biomaterial scaffold with biological cues to direct the cellular repair.**

53 Kon E, Filardo G, Di Martino A, Marcacci M. ACI and MACI. *J. Knee Surg.* 25(1), 17–22 (2012).

54 Munirah S, Samsudin OC, Chen HC, Salmah SH, Aminuddin BS, Ruszymah BH. Articular cartilage restoration in load-bearing osteochondral defects by implantation of autologous chondrocyte-fibrin constructs: an experimental study in sheep. *J. Bone Joint Surg. Br.* 89(8), 1099–1109 (2007).

55 Kon E, Delcogliano M, Filardo G *et al.* Orderly osteochondral regeneration in a sheep model using a novel nano-composite multilayered biomaterial. *J. Orthop. Res.* 28(1), 116–124 (2010).